Structure-property relationships in glass reinforced polyamide: 1) The effects of fibre content.

J. L. Thomason

Abstract

We present the results of an extensive study of the performance of injection moulded glass-fibre reinforced polyamide 66 with glass content between 0-40% and based on two chopped glass products both sized with polyamide compatible sizing. Mechanical properties generally improved with increasing glass content, modulus linearly, strength with a maximum at 40-50% glass content, and impact showing an initial decrease from the resin value with a minimum at 4% glass content before increasing at higher glass contents. Residual fibre length decreased linearly with increasing glass content. Interfacial strength was found to be in the 30-36 MPa range and no significant differences in dry as moulded performance was found between the 123D and 173X sizings. Conditioning these composites in either boiling water or water/glycol mixtures leads to a dramatic drop in both tensile modulus and tensile strength. This is most likely due to the high level of matrix plasticization. After conditioning the 173X sized glass delivered a significantly higher level of tensile elongation at all fibre contents. Excellent agreement was obtained between the experimental data and the theoretical predictions of the Cox model for modulus and the Kelly-Tyson model for strength over the range of fibre concentrations studied.

Introduction

Glass reinforced thermoplastics continues to be one of the most exciting growth areas in the composites market. In recent years there has been an increasing growth in the use of glass-fibre-thermoplastic composite systems in semi-structural and engineering applications. These thermoplastic matrix composite systems combine ease of processing with property advantages such as enhanced toughness and an unlimited shelf life. Furthermore, their intrinsic recyclability is rapidly being recognised as a strong driving force for their further application. Their potential for high-volume processing combined with high levels of end use property levels and associated lower manufacturing costs has spurred the current expansion of research and development activities on thermoplastic matrix composites. Parallel to this growth has been the increasing recognition of the need to better understand and measure the micro-mechanical material parameters and processing parameters which control the performance of such composite parts. Glass fibre reinforced polyamides are excellent composite materials in terms of their high levels of mechanical performance and temperature resistance. However, the mechanical properties of polyamide based composites decrease markedly upon the absorption of water and other polar fluids. The mechanical performance of these composites results from a combination of the fibre and matrix properties and the ability to transfer stresses across the fibre-matrix interface. Variables such as the fibre content, diameter, orientation and the interfacial strength are of prime importance to the final balance of properties exhibited by injection moulded thermoplastic composites (1-8). The optimisation of composite processibility and performance through control of the base materials and the various steps of fibre-matrix combination and parts production is already a major technical challenge. The challenge to a fibre reinforcement supplier is how to offer outstanding reinforcement products which can meet the demands of all the intermediaries in the composite chain and match the internal manufacturing and financial targets.

For some time we have been engaged in a programme to further elucidate the structure-processing-property relationships in glass fibre reinforced thermoplastics. In this report we present an in depth discussion of the results on of a number of trials of short glass fibre reinforced polyamide 66. We present results on injection moulded composites manufactured with a range of glass contents (0-40 % wt) and two sizing chemistries for polyamide reinforcement. Mechanical performance has been determined for both "dry as moulded" state and after hydrolytic and temperature conditioning. We discuss the effects of fibre length, fibre orientation and interfacial strength and compare a number of theoretical models against the experimental data.

Experimental

The E-glass samples, 123D-10C and 173X-10C, used in this study were all produced using the Owens Corning Cratec® process for chopped strands (9). These samples were chopped to a length of 4 mm and the individual fibres had a nominal average diameter of 10 μm. Both samples were coated with sizings which are design for polyamide reinforcement. 123D is a typical sizing designed to maximise the "dry as moulded" (DaM) performance of glass reinforced polyamides where the main ingredients are aminosilane coupling agent and a commercial polyurethane dispersion (10,11). 173X sizing contains some extra components, including the homopolymer of an acrylic acid monomer, which enhance the retention of composite mechanical properties in elevated temperature hydrolytic environments (12,13). The polyamide 6,6 (PA6,6) used was DuPont Zytel 101. The glass bundles and pre-dried PA6,6 pellets were dry blended by weight to the appropriate glass content and

2

compounded on a single screw extruder (2.5 inch, 3.75:1, 24:1 L/D screw). The compounds were moulded into test bars on a 200-ton Cincinnati Milacron moulding machine. Set point temperatures were 288-293°C for compounding and 293-299°C for moulding, at a mould temperature of 93°C. Hydrolysis conditioning took place in a temperature controlled a self-pressurising vessel with samples fully immersed in a 50:50 mixture of water and glycol. On removal from conditioning container samples were cooled to room temperature in a bath of 50/50 water/glycol, then stored in plastic bags for immediate mechanical testing. Three series of extrusion and moulding trials were carried out;

Series A   covering 0-40% w/w of 123D-10C
Series B1   covering 10-40% w/w of 173X-10C
Series B2   covering 0-10% w/w of 173X-10C

Tensile properties were measured in accordance with the procedures in ASTM D-638, using ASTM Type I specimens at a crosshead rate of 5 mm/min (0.2 inches/min) and an extensometer gauge length of 50 mm (2 inches). Flexural properties were measured in accordance with the procedures in ASTM D-790, at a crosshead rate of 2.5 mm/min (0.1 inches/min) and a span width of 50 mm (2 inches). Izod and modified Charpy impact properties were measured on ten specimens in accordance with the procedures in ASTM D-256 and ASTM D-4812. DTUL was measured on three specimens of each sample according to ASTM D648. Unless otherwise stated, all mechanical property testing was performed at 23°C and at a relative humidity of 50%. Fibre length and diameters were determined by image analysis and optical microscopy on fibre samples removed from the moulded bars after high temperature ashing. Measurement of fibre orientation was carried out on cross sections of a moulded tensile bars was cut perpendicular to the flow direction. The sections were polished and a series of optical micrographs was taken systematically across the thickness of the bar. The orientation of any fibre can be determined from its elliptical profile using the equation (14,15)

$$\cos(\phi) = W/L = 4A/\pi L^2 \tag{1}$$

where ϕ is the angle the fibre axis makes with the flow direction, W is the minor axis of the ellipse which should also represent the fibre diameter, L is the ellipse major axis, and A is the area of the ellipse. Either of possibilities in equation 1 may be used, however it has been shown (15) that the greatest experimental error comes form the measurement of W and that the area method produces values with a lower degree of uncertainty. The Hermans orientation parameter (f_p) can be calculated from this data using

$$f_p = 2 < \cos^2(\phi) > -1 \tag{2}$$

where the average value of $<\cos^2 \phi>$ is approximated by

$$< \cos^2(\phi) > = \Sigma_i [N(\phi_i) \cos^2(\phi_i)] / \Sigma_i [N(\phi_i)] \tag{3}$$

The values of $N(\phi_i)$ must first be adjusted (16) by dividing by $\cos(\phi_i)$ due to the lower probability of the section crossing fibres with higher values of ϕ ωηερε ϕ is the angle between the fibre axis and the reference direction (commonly the injection flow direction). The average fibre orientation factor (η_o) used in the Cox-Krenchel theory for composite modulus can be calculated using (17,18)

$$\eta_o = <\cos^4(\phi)> \tag{4}$$

Results

The results for the tensile moduli as a function of fibre concentration are shown in Figure 1, the error bars represent the 95% confidence interval for the mean values. It can be seen that the stiffness of these mouldings increases almost linearly with increasing fibre weight fraction up to the 40% w/w level. There is no systematic difference in composite moduli observed between Series A and Series B. Despite the fact that most practical mouldings are mixed according to weight fractions, analysis of composite properties is normally carried out considering fibre volume fraction since most underlying structure-performance are related to volume fraction. As shown in Figure 2, the data from both series can be superimposed on one plot of modulus versus glass fibre volume fraction and an excellent straight line fit can be obtained with the data.

The results for the Tensile and Flexural Strength as a function of fibre concentration are shown in Figure 3. In all data sets it can be seen that, at low fibre loading, the strength of these mouldings also increases linearly with increasing fibre concentration. However, at higher fibre loading (above 25% w/w) there appears to be some deviation from linearity, particularly in the Flexural Strength data. Once again there is no systematic difference in composite performance observed between Series A and Series B. The combined data for both series are shown versus fibre volume fraction in Figure 4. The non-linearity of the strength versus fibre content relationship is made clear in this Figure by the fitting of polynomial curves. The third order polynomial gives a slightly better fit over the full range of fibre content. It is interesting to note that both polynomials predict a maximum in strength between 40-50% w/w (0.23-0.31 v/v). This trend for an apparent maximum in composite strength versus fibre content has been observed in a number of injection-moulded glass-reinforced thermoplastics. The results for the tensile elongation as a function of fibre concentration are shown in Figure 5. It can be seen that the addition of even very low levels of reinforcement leads to a very large reduction in the ductility of the material. The elongation continues to fall with increasing fibre content in the 2-10% range. From 10-30% the elongation is approximately constant and then above 33% it starts to fall again as the fibre content is increased. There is a small but significant difference in the performance of Series A and B in tensile elongation in the 10-40% glass content range and a paired t-test analysis shows that this difference is significant at the 95% confidence level.

The results for the notched and unnotched Izod Impact as a function of fibre concentration are shown in Figures 6-7. The influence of fibre content on the impact performance is clearly more complex and we must be careful to discriminate between the notched and unnotched test configuration. The notched Izod data from both series are compared in Figure 6 where a linear relationship with glass content is clearly seen above 5%wt reinforcement level. Furthermore there is some indication in Figure 6 that 123D sizing systematically gives slightly better DaM notched Impact performance than 173X sizing. A paired t-test analysis shows that this difference is significant at the 95% confidence level. It should be noted that the values at zero glass content are well above the trend lines for samples containing glass, which suggests that the impact behaviour of PA66 is radically altered by the addition of glass fibres. This is probably a reflection of the notch sensitivity of polyamides. Consequently the addition of fibres only has a beneficial effect on notched Izod above 10% w/w. The addition of small amounts of fibre has a drastic effect on the unnotched impact and even at 40% w/w loading we do not recover the initial performance of the

PA66. It can also be seen in Figure 7 that the unnotched data are better fitted by a third order polynomial. The unnotched impact resistance of the PA66 resin itself is very high and gave "no breaks" in the test. The addition of a small concentration of glass fibre leads to a sharp fall in the unnotched impact resistance with a minimum value at approximately 4 wt%. Above this concentration the impact resistance increases slowly up to approximately 20 wt% concentration and then exhibits a steep rise between 20-30%. Above 30% the impact resistance continues to rise but at a much reduced rate. There is no significant difference observed in the unnotched impact performance of the two series.

The elevated temperature performance of a structural composite is an important consideration and is often judged by the deflection temperature under load (DTUL). The DTUL data versus glass content are shown in Figure 8. It can be seen that addition of even small amounts (10% w/w) of glass fibre raise the DTUL from the resin value around 75°C to above 245°C. As the fibre content is further increased there is a small but significant increase in DTUL. However, it is clear that the values are approaching a plateau level, which is defined by the melting point of the PA66 (around 265°C). There is no significant difference in DTUL performance between series A and series B.

The results of the tensile testing of the boiling water conditioned samples are summarised in Figures 9-11. In Figure 9 the plasticizing effect of water on PA66 and its composites is clearly shown. The resin modulus is reduced by 80% and this has a significant effect on the modulus of the composites with a reduction of 65-45% observed over the range of glass fibre content in this study. Despite this significant reduction in performance, the linear relationship between modulus and fibre volume fraction is still evident in the conditioned samples. Furthermore, there is no evidence of a significant difference in the modulus of Series A and B after this short term conditioning. In a similar vein the results for tensile strength after boiling water conditioning show a large reduction in comparison to the DaM results. In this case the reduction in performance is in the range of 45-50% for all the samples. It is interesting to note that, at higher glass fibre contents, we do see some evidence for a difference in performance between Series A and B with 173X sizing leading to a greater retention of strength after conditioning. The results for tensile elongation after boiling water conditioning are compared with DaM results in Figure 11. These data clearly show the plasticising effect of this conditioning on these composites. The composite elongation shows a large increase after conditioning, particularly in samples with higher resin content. The plasticizing effect of moisture is well known in polyamide based materials. It is interesting to note that the two sizings show a clear difference in performance after conditioning with 173X sizing delivering a higher level of tensile elongation at all fibre contents.

The performance of series B1 after hydrolysis conditioning is summarised in Figures 12-14 and compared with the dry and the 24 hour boiled samples. It can be seen in Figure 12 that all conditioned samples show a significantly lower modulus compared with the dry samples. It can be noted that the data for the 24 hour water boil and the 200 hour and 500 hour water-glycol treatment at 120°C show no significant differences across the full range of fibre content studied. Interestingly the modulus after 1000 hours water-glycol treatment appears to increase compared to the other conditioned samples. Indeed, at higher glass contents, there already appears to be a trend for higher modulus after 500 hours treatment. Furthermore it can be seen that the slope of the trend-lines of modulus versus volume fraction of all the conditioned samples are approximately equal and are significantly lower than the slope of the line for the data from the dry as moulded samples. The results for tensile strength in Figure 13 show some similar trends as observed for modulus. All the conditioned samples show significantly lower performance compared to the dry samples. There is

little significant differences observed between the strength performance of the 24 hour water boiled and 200 hour and 500 hour water-glycol conditioned samples. However, we get significant changes when we go to 1000 hour water-glycol conditioning with a further significant drop in performance. The tensile elongation data are shown in Figure 14. This figure reveals the high level of plasticisation of the polyamide matrix caused by the conditioning in an aqueous environment.

It is well known that the processing of glass fibres into injection moulded composites leads to large reductions in the fibre length (7,19-21). Figure 15 shows both number average (L_n) and weight average (L_w) length versus fibre concentration for both series of composites. It can be seen that the 4 mm fibres used in this study were reduced to less than 0.7 mm by the compounding and moulding process. It is also clear that the glass content plays a role in determining the residual composite fibre length. Below 10 %wt fibre content the final average fibre length appears to be independent of the fibre concentration. In the range of 10-40 %wt. of fibres there is little significant difference between the two series with different fibre sizings and there is an approximately linear decrease of both length averages with increasing fibre content. This is likely due to the fact that increased fibre loadings leads to increased probability of fibre-fibre and fibre-machine interaction (and resultant fibre damage) and an increased apparent melt viscosity resulting in higher bending forces on the fibres during compounding and moulding. This decrease in residual fibre length with increasing fibre concentration may well be an important factor in the explanation of why the strength based properties of these composites show a decreasing reinforcing effect as the fibre concentration is increased. In Figure 16 the weight average fibre length in the injection moulded bars is compared with that of the fibres in the extruded pellets, prior to moulding, for series A. It can be seen from this data that a large part of the final length reduction has taken place during the compounding step. It is interesting to note that the slope of both lines is approximately equal implying that the mechanism of fibre length degradation is similar in both processes.

The average fibre orientation factors for $< \cos^2(\phi) >$ and for $< \cos^4(\phi) >$ obtained using the optical analysis method are shown in Figure 17. These results confirm the high level of fibre orientation parallel to the flow direction in these injection moulded samples. In this case there appears to be an increase in the average orientation of the fibres as the glass content is increased from very low values. This is similar to the trend previously reported (22). Although the data in Figure 17 appears to show a maximum in average orientation factor in the 20-30% wt region it should be realised that the data is only representative of a small area of the cross section of the samples (23). It seems more realistic to say that the orientation factors appear to be approximately constant at $< \cos^2(\phi) > = 0.72$ and $< \cos^4(\phi) > = 0.55$ in the commercially important range of glass contents (10-40% wt).

Discussion

The data for the composite tensile modulus in Figure 1 can be modeled using a number of approaches. One common approach is to use a simple "rule-of-mixtures" equation

$$E_c = \eta_0 \eta_l V_f E_f + (1 - V_f) E_m \qquad (5)$$

Where Ef is the fibre modulus, Em is the matrix modulus, Vf is the fibre volume fraction, η_o is a factor which modifies the fibre contribution in proportion to the fibre orientation relative to the loading direction and η_l is a factor which modifies the fibre contribution in proportion to the

average fibre length. We can use the fibre length data reported in Figure 15 to calculate the η_l factor using the Cox shear lag method (17). Combining these values with the experimental values of composite and matrix modulus we can obtain a value for the orientation parameter (η_o) for each glass content (18).

Another approach is to use the equation

$$E_c = \eta_0 E_1 + (1 - \eta_0) E_2 \tag{6}$$

where E_1 and E_2 are obtained from the Halpin-Tsai equations (24) for the modulus of a unidirectionally reinforced laminate.

$$E_j = E_m \left[\frac{1 + \xi_j \eta_j V_f}{1 - \eta_j V_f} \right] \qquad \eta_j = \frac{\left(E_f / E_m \right) - 1}{\left(E_f / E_m \right) + \xi_j} \qquad \xi_1 = \frac{2L}{D} \qquad \xi_2 = 2 \tag{7}$$

where L/D is the fibre length to diameter ratio. We have calculated values for η_o for the Series B samples using the above two methods and the values of Young's modulus obtained from both tensile and flexural testing. We observed that the values of η_o obtained from equations 5 and 6 were very similar, furthermore the values obtained from the two test methods were also similar. Given the similarity of the results and the potential level for error in these η_o values we felt that it was acceptable to average the values obtained for any given sample. This enables us to compare the fibre orientation factor obtained from analysis of the composite modulus with those obtained by the optical method.. It is clear from the results shown in Figure 18 that the best agreement between the modulus and the optical method is obtained when considering $\eta_o = <\cos^2(\phi)>$ from the optical method.

Krenchel (18) showed that η_o in the Cox modulus model (equation 5) can be calculated from $\eta_o = <\cos^4(\phi)>$ and this has been used with some success in modeling the stiffness of composites (25-27). However it can be seen in Figure 18 that these values fall well below the values calculated using equation 5, which we have observed and reported previously (7, 22). The possible causes for these apparently conflicting results may lie either in error in the experimental measurements or in the assumptions behind the equations use in the calculation of η_o. The measurement of the Young's modulus can be assumed to be fairly accurate; however there are a number of issues related to the assumptions made using this method. For instance the assumption that the modulus of the unreinforced resin can be substituted for the composite matrix modulus becomes more questionable as the fibre content increases. As discussed previously (23, 28, 29) there are numerous mechanisms by which the presence of the fibres can modify the properties of the polymer matrix in their vicinity. Clearly as the fibre content is increased the relative volume fraction of the resin which could be affected by interaction with the fibres increases rapidly. This could consequently lead to an increasing level of error in the calculation of η_o using this method. There is also much discussion about the r/R factor used in the shear lag theory where r is the fibre radius and R is related to the mean spacing of the fibres. The r/R factor can be related to the fibre volume fraction by assumption of a certain fibre packing arrangement. It is likely that these assumptions may also become more questionable as the fibre content increases. At very low fibre content the method based on equation 5 uses the difference of two values (E_c and E_m) which are relatively close together and therefore any

errors in the measurements or calculation of the various factors can lead to increasingly large error in the final values of η_o. The Halpin-Tsai equations are known to fit some data very well at low fibre volume fractions, but to under-predict stiffness at high volume fractions which might lead to artificially low values for η_o at high fibre contents. Tucker and Liang have recently reviewed the assumptions inherent in a number of the models for composite stiffness (30). On the positive side, the modulus method does give a true average for η_o over all the fibres in the sample. Conversely, the optical method, like most microscopy techniques, only measures a very small proportion of the fibres in each sample. In our case we examined approximately 1.5% of the total cross sectional area of the sample.

We can apply a similar analysis to the data on the modulus of the conditioned samples in Figure 11. One might assume in the first instance that the average fibre orientation factor of the various samples would not be significantly altered by the conditioning process. If that were the case then we should obtain similar values for η_o for each sample for each condition. It is interesting to note in Figure 19, which shows an intermediate step in the analysis where we have deducted the matrix contribution to the composite modulus, that the data for all the conditioned samples collapses onto a single line. This indicates that the fibre contribution to the composite modulus is identical in all cases and that the differences observed must be principally due to differences in the state of the matrix. The results for the analysis of for η_o from the conditioned samples using calculations based on equation 5 are shown in Figure 20. The data appears to show that η_o is systematically reduced as we increase the level of conditioning of these composites. As stated above this seems to be most unlikely to reflect the physical reality of the situation. In a more detailed study (31) on the physical effects of this type of conditioning on injection moulded samples we have ascertained that the volume of polyamide 66 increases by 12-15% during conditioning. Assuming that no volumetric change takes place in the glass fibres this swelling of the matrix would lead to reduction in the actual volume fraction of fibres in each sample. When we use these modified values of fibre volume fraction in the above calculations we obtain the results for η_o shown in Figure 21. In this Figure we can see that four from the five data sets can be consider approximately identical and only the values for the 1000 hours hydrolysis conditioning still differ from the others. It is also worth noting at this point that the results of this orientation factor analysis carried out on the data in Figure 11 using an approach based on equation 6 we obtain many values greater than unity, which is a physical impossibility. Correcting for the actual fibre volume fraction in the samples did not improve the results in this case. Furthermore, as can be seen from the results shown in Figure 22, we did not obtain any agreement between the values of η_o from the five data sets. It would therefore appear that the Halpin-Tsai approach is not particularly well suited for this type of analysis in injection moulded composites.

The macro-method analysis used here to obtain values of the interfacial shear strength (IFSS) was originally proposed by Bowyer and Bader (32,33) and an improved version has been extensively reviewed by Thomason (22,34-36). The macro-method has an enormous attraction in that it utilises data which are readily available from standard composite mechanical testing and requires only an extra determination of fibre length distribution, which is a common characterisation tool of those working with discontinuous fibre composites. The method is based on the Kelly-Tyson model for the prediction of the strength (σ_{uc}) of a polymer composite reinforced with discrete aligned fibres (37). This model can be simplified to $\sigma_{uc} = \eta_o (X + Y) + Z$, where Z is the matrix contribution, X is the sub-critical fibre contribution, and Y is the super critical contribution, in reference to a critical fibre length defined by $L_c = \sigma_{uf} D / 2\tau$ where σ_{uf} is the fibre strength, D is the average fibre diameter

8

and τ is the IFSS. The Kelly-Tyson model assumes that all the fibres are aligned in the loading direction and the equation cannot be integrated to give a simple numerical orientation factor to account for the average fibre orientation. The common approach to this problem is to fit the experimental data using a simple numerical orientation factor (η_o). Bowyer and Bader extended the original Kelly-Tyson concept to model the stress-strain curve of the composite *prior* to failure (32,33). The basis of their argument was that at any strain value (ε_c) there exists a critical fibre length $L_\varepsilon = \sigma_f.D / 2\tau$. Fibres shorter than L_ε carry an average stress $= L.\tau /D$ and fibres longer than L_ε carry an average stress $= E_f \varepsilon_c(1-(E_f \varepsilon_c D/4L \tau)$. The composite stress at any strain level may then given by

$$\sigma_c = \eta_0 \left(\sum_i \left[\frac{\tau L_i V_i}{D} \right] + \sum_j \left[E_f \varepsilon_c V_j \left(1 - \frac{E_f \varepsilon_c D}{4\tau L_j} \right) \right] \right) + \left(1 - V_f \right) E_m \varepsilon_c \tag{8}$$

Although η_o and τ are not generally known, values for these factors can be obtained if the composite stress (σ_1 and σ_2) at two strain values (ε_1 and ε_2) are known. The matrix contribution Z was calculated from an independent matrix modulus determination and used to calculate the ratio R of the fibre contributions at the two strains

$$R = \frac{\sigma_1 - Z_1}{\sigma_2 - Z_2} \qquad R* = \frac{X_1 + Y_1}{X_2 + Y_2} \tag{9}$$

Equation 6 was then used with an assumed value of τ to calculate the ratio R*, the theoretical value of R. At this point the ratios R and R* are independent of η_o. The value of τ is then adjusted until R*=R and that value of τ is used in Equation 6 to obtain a value for η_o (which is assumed to be the same at both strain levels).

Thomason has recently shown how the model can be improved by taking into account the non-linear stress-strain behaviour of thermoplastic matrices (22,34-36). For the matrix used in this study the stress contribution (in MPa) can be calculated for any strain level between 0-3% using

$$\sigma_{PA} = -0.56\varepsilon^3 - 0.55\varepsilon^2 + 28.85 \varepsilon \tag{10}$$

Furthermore the analysis method was extended to obtain a value for σ_{uf} the maximum fibre stress at composite failure. This can be obtained by inserting the composite breaking stress into the original Kelly-Tyson equation along with the determined values of τ and η_o. Consequently, this method gives a complete characterisation of the micromechanical parameters η_o, τ, σ_{uf} of any system. The relative simplicity and cost effectiveness of this approach makes it ideal as an industrial screening tool for product developers. When the stress at the 1% and 2% strain levels obtained from tensile testing are combined with the full fibre length distributions used to obtain the averages in Figure 15 and applied in the procedure described above we obtain values for the parameters η_o, τ, σ_{uf}.

The results for η_o as a function of glass content obtained using this method are shown in Figure 23 where they are compared with values for average fibre orientation parameter obtained from back calculation using the composite modulus shown in Figure 18. Not surprisingly the macro-analysis values, which also use input data from mechanical testing, follow a similar trend to those obtained from the composite modulus.

The results for the IFSS are shown in Figure 24. The data appear to be scattered about a line of decreasing IFSS with increasing fibre content. The data shows no significant difference, using a paired T-test at the 95% confidence level, between the IFSS of series A and B. The solid line shown in Figure 24 is obtained from a least squares regression analysis for all data and a statistical analysis showed that both the constant and the coefficient are statistically significant at the 95% confidence level. Therefore, despite the scatter in the data, it appears that that the IFSS does decrease with increasing fibre content. This general trend for a decrease in the apparent IFSS with increasing fibre content has been observed previously for injection moulded short fibre reinforced thermoplastics over this range of fibre contents (10-40 wt%) (22,34-36).

The IFSS – fibre content relationship has been compared to a similar trend in the calculated values of residual compressive radial stresses on the fibres in these systems. These interfacial compressive stresses are a result of the differential in thermal expansion coefficients between the inorganic fibres and the organic polymer matrices. Calculation of a "frictional" interfacial strength contribution from the radial stress requires modifying the values with a coefficient of friction between fibre and matrix of the order of 0.4 – 0.7 depending on the resin matrix. Although this might appear to be a relatively large value, it should be noted that we are referring to a static coefficient of friction which can be significantly higher than the more common dynamic value. Schoolenberg (38) has shown that the apparent IFSS in single fibre pullout testing of glass fibre and polypropylene can be explained fully by the static friction due to the interfacial compressive stresses and a static friction coefficient of 0.65. The dotted line in Figure 24 shows such predictions using a coefficient of friction of 0.6 and radial stress values calculated using the equations proposed by Nairn (39). It can be seen that it is possible to obtain a reasonable fit to the experimental data using this method however it is questionable whether we can accept an IFSS with polyamide that is only dependent on residual stresses. Polyamide has a much greater possibility for chemical and physical interaction with the glass fibre than polypropylene and it seems likely that there are other contributions to the apparent IFSS with polyamide.

Previous results using this macro-model analysis has shown an excellent correlation between the output value of the fibre stress at composite failure σ_f and the experimental tensile elongation at failure. In Figure 25 we show strain value calculated from σ_f and fibre modulus $E_f = 72$ GPa plotted against the experimental values. Once again we see an excellent correlation, which indicates that fibres which are longer than Lc (and are aligned with the loading direction) are strained to approximately the same level as the composite itself. Figure 26 compares the values for composite strength obtained from the Kelly-Tyson theory with the experimental tensile strengths. As input we have used the full fibre length distributions, the orientation parameter obtained from analysis of the composite modulus, IFSS calculated using the regression line in Figure 25 with the composite fibre weight fraction, the experimental strain at failure, and the resin contribution calculated using equation 10. It can be seen that we obtain a good fit between theory and experiment.

Conclusions

This study of the "dry as moulded" performance of injection moulded glass-fibre reinforced polyamide 66 has revealed that the modulus of these mouldings increases linearly with fibre content between 0-40% w/w. In this glass content range there were no significant differences in modulus detected due to the different sizing chemistries studied. Excellent agreement between the experimental data and the theoretical predictions of the Cox model was obtained over the range of fibre concentrations studied. In terms of tensile and flexural strength we also obtained a linear relationship at lower glass contents (below 25% w/w). However, at higher fibre loadings there appears to be some deviation from linearity, particularly in flexural strength. This indicated a decreasing return in composite performance improvement with increasing glass content. A least squares fit of the data with a polynomial function predicts a maximum in composite strength between 40-50% w/w of glass fibres. No significant difference in strength performance was detected between the 123D and 173X sizing chemistries although the 173X chemistry did deliver a small but significant increase in tensile elongation in the composites.

Both notched and unnotched Izod impact resistance increased with glass content in the 10-40% w/w range. The notched Izod data were approximately linear with glass content, the unnotched data were better fitted by a third order polynomial reflecting the direct relationship with composite strength. For both types of impact there is an initial decrease from the resin values on addition of glass. Notched Izod requires more than 10% w/w fibre addition to reach values higher than the resin. However, even at 40% w/w fibre content the unnotched impact performance is still lower than the resin alone. At very low glass content the minimum in both notched and unnotched Izod occurred at approximately 4% w/w glass content. There is some evidence in the data that the 123D sizing chemistry gives slightly improved impact resistance. The deflection temperature under load of PA66 is improved dramatically by the addition of only low levels of glass. Above 10% w/w there is some further improvement but this levels out as the PA66 melting temperature is approached.

Conditioning these composites in either boiling water for 24 hours or water/glycol mixtures at 120°C for much longer times leads to a dramatic drop in both tensile modulus and tensile strength. This is most likely due to the high level of matrix plasticization. After conditioning the 173X sized glass delivered a significantly higher level of tensile elongation at all fibre contents. The average residual fibre length in the moulded composites decreased approximately linearly in the 10-40% fibre content range. It was shown that the largest proportion of the fibre length reduction took place during the extrusion compounding step.

There were some differences in the results between average fibre orientation parameters calculated using composite modulus analysis and optical analysis of composite cross sections. Deeper investigation of the modulus based method, particularly with conditioned samples, indicated that the Halpin-Tsai approach is not suited for this type of analysis in injection moulded composites. The interfacial shear strength was found to be in the range of 30-36 MPa for composites in the "dry as moulded" state. No significant difference in the "dry as moulded" interfacial strength was detected between the two sizing systems investigated. Using values for the interfacial strength and fibre average orientation in the Kelly-Tyson equation it was possible to obtain an excellent fit between calculated composite tensile strengths and the experimental data.

References

1. Sato N, Kurauchi T, Sato S, and Kamigaito O. Mechanism of fracture of short glass fibre-reinforced polyamide thermoplastic. J. Mater. Sci. 1984:19;1145-1152

2. Sato N, Kurauchi T, Sato S, and Kamigaito O. Reinforcing mechanism by small diameter fiber in short fiber composites. J. Compos. Mater. 1998:22;850-873

3. Horst JJ, and Spoormaker JL. Fatigue fracture mechanisms and fractography of short-glass fibre-reinforced polyamide 6. J. Mater. Sci. 1997:32;3641-3651.

4. Akay M., Barkley D. Fibre orientation and mechanical behaviour in reinforced thermoplastic injection mouldings. J.Mater. Sci. 1991;26:2731-42

5. Laura DM, Keskkula H, Barlow JW, Paul DR. Effect of glass fiber surface chemistry on the mechanical properties of glass fiber reinforced, rubber-thoughened nylon 6. Polymer 2002:43;4673-4687

6. Thomason, J.L., Vlug, M.A., Schipper, G. and Krikor, H.G.L.T. The influence of fibre length and concentration on the properties of glass fibre reinforced polypropylene: 3) Strength and strain at failure. Composites 1996;27A:1075-1084.

7. Thomason, J.L. and Vlug, M.A. The influence of fibre length and concentration on the properties of glass fibre reinforced polypropylene: 4) Impact properties. Composites 1997:28A;277-288 .

8. Thomason J.L., "The influence of fibre properties of the performance of glass-fibre-reinforced polyamide 6,6.", Compos.Sci.Technol. 1999;59:2315-2328

9. Campbell LE, in "Handbook of Polypropylene and Polypropylene Composites", ed. H.G. Karian, Marcel Dekker, New York, 1999

10. United States Patent 4,255,317

11. Thomason, J.L. and Adzima, L.J. Sizing up the interface: an insider's guide to the science of science. Composites Part A 2001;32:313-321.

12. United States Patent 5,236,982

13. United States Patent 6,365,272

14. Toll, S. and Andersson, P. O. Microstructure of long- and short-fibre reinforced injection moulded polyamide. Polym.Composites 1993;14:116-125.

15. Toll, S. and Andersson, P.O. Microstructural characterization of injection moulded composites using image analysis. Composites 1991;22:298-306.

16. Bay RS, Tucker CL. Polym. Eng. Sci., **32**, pp240-253 (1992) "Stereological measurement and error estimates for three-dimensional fiber orientation"

17. Cox HL. "The elasticity and strength of paper and other fibrous materials. Brit.J.Appl.Phys. 1952;3:72-79

18. H. Krenchel in "Fibre Reinforcement", Akademisk Forlag, Copenhagen, (1964)

19. Thomason, J.L. The influence of fibre length and concentration on the properties of glass fibre reinforced polypropylene: 5) Injection moulded long and short fibre PP. Composites 2002;33A:1641-1652.

20. Franzen B, Klason C, Kubat J, Kitano T. Fibre degradation during processing of short fibre reinforced thermoplastics. Composites 1989;20:65-76.

21. Bailey RS, Kraft H. A study of fibre attrition in the processing of long fibre reinforced thermoplastics. Intern. Polymer Processing, 1987;2:94-101.

22. Thomason, J.L. Micromechanical Parameters from Macromechanical Measurements on Glass Reinforced Polyamide 6,6. Compos.Sci.Technol., 2001:61:2007-2016

23. Thomason, J.L.. The influence of fibre length and concentration on the properties of glass fibre reinforced polypropylene: 6) The properties of injection moulded long fibre PP at high fibre content. Composites 2005;36A:995-1003.
24. Halpin JC, Kardos JL. The Halpin-Tsai equations: A review. Polym.Eng.Sci. 1976;16:344-52.
25. Thomason JL, Vlug MA. The influence of fibre length and concentration on the properties of glass fibre reinforced polypropylene: 1) Tensile and Flexural Modulus. Composites 1996;27A:477-84.
26. Rosenthal J. A model for determining fiber reinforcement efficiencies and fiber orientation in polymer composites. Polym.Compos. 1992:13:462-466
27. Robinson IM, Robinson JM. Review of the influence of fibre aspect ratio on the deformation of discontinuous fibre-reinforced composites. J.Mater.Sci. 1994:29:4663-4677
28. Thomason JL, Van Rooyen AA. Transcrystallized interphase in thermoplastic composites. J Mater Sci 1992;27:889-907
29. Thomason JL. The interface region in glass-fibre-reinforced epoxy resin composites: Part 3 Characterisation of fibre surface coatings and the interphase. Composites 1995;26:487-498
30. Tucker CL, Liang E. Stiffness predictions for unidirectional short-fiber composites: Review and evaluation. Compos.Sci.Technol. 1999;59:655-71.
31. Thomason JL. Submitted to Polymer Composites 2005.
32. Bader MG, Bowyer WH. An improved method of production of high strength fibre reinforced thermoplastics. Composites 1973;4:150-6
33. Bowyer W.H. and Bader M.G. On the reinforcement of thermoplastics by perfectly aligned discontinuous fibres. J. Mater. Sci., 1972, 7, 1315-1321.
34. Thomason JL. Interfacial Strength in Thermoplastic Composites – At Last an Industry Friendly Measurement Method ? Composites Part A 2002;33:1283-8.
35. Thomason JL. Micromechanical Parameters from Macromechanical Measurements on Glass Reinforced Polypropylene. Compos.Sci.Technol. 2002;62:1455-68.
36. Thomason JL. Micromechanical Parameters from Macromechanical Measurements on Glass Reinforced Polybutyleneterepthalate. Composites Part A 2001;33:331-39
37. Kelly A, Tyson WR. Tensile properties of fibre-reinforced metals. J.Mech.Phys.Solids, 1965;13:329-50.
38. .Schoolenberg GE. Some wetting and adhesion phenomena in polypropylene composites. Chapter 3.6 in "Polypropylene: Structure, blends and composites" Edited by J.Karger-Kocsis, Chapmann and Hall, London 1995
39. Nairn JA. Thermoelastic analysis of residual stresses in unidirectional, high-performance composites. Polym. Compos. 1985;6:123-30.
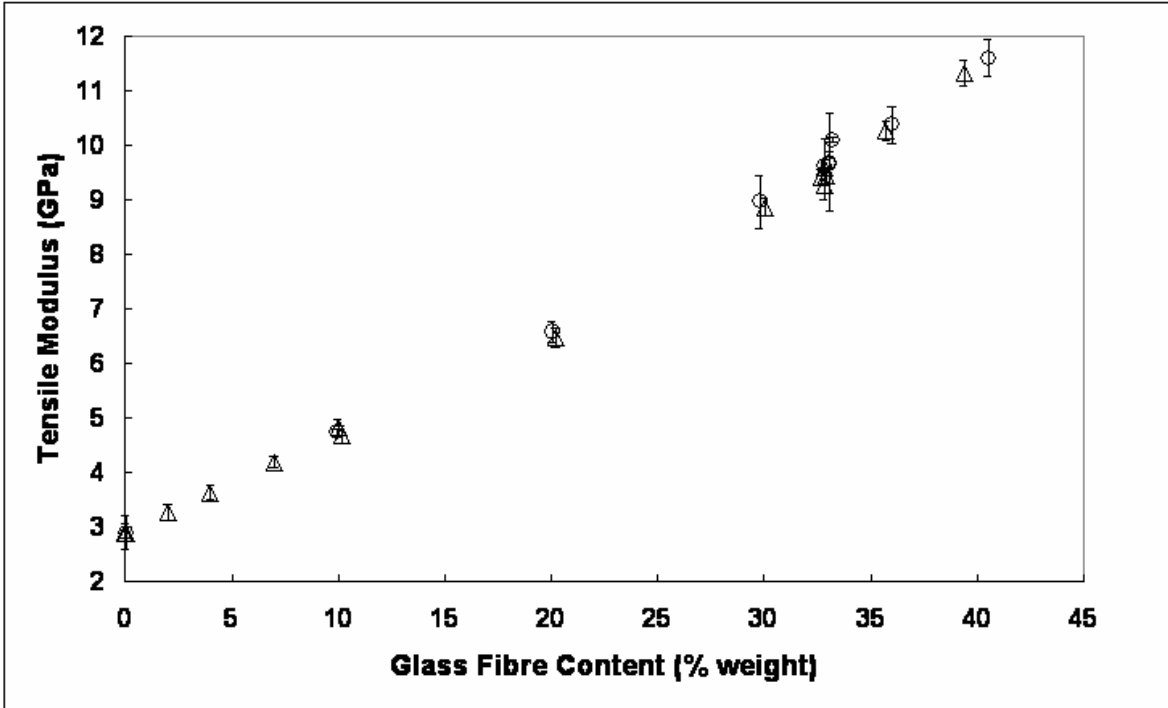
Figure 1 Tensile Modulus vs Fibre Weight Content (○ series A, △ series B)
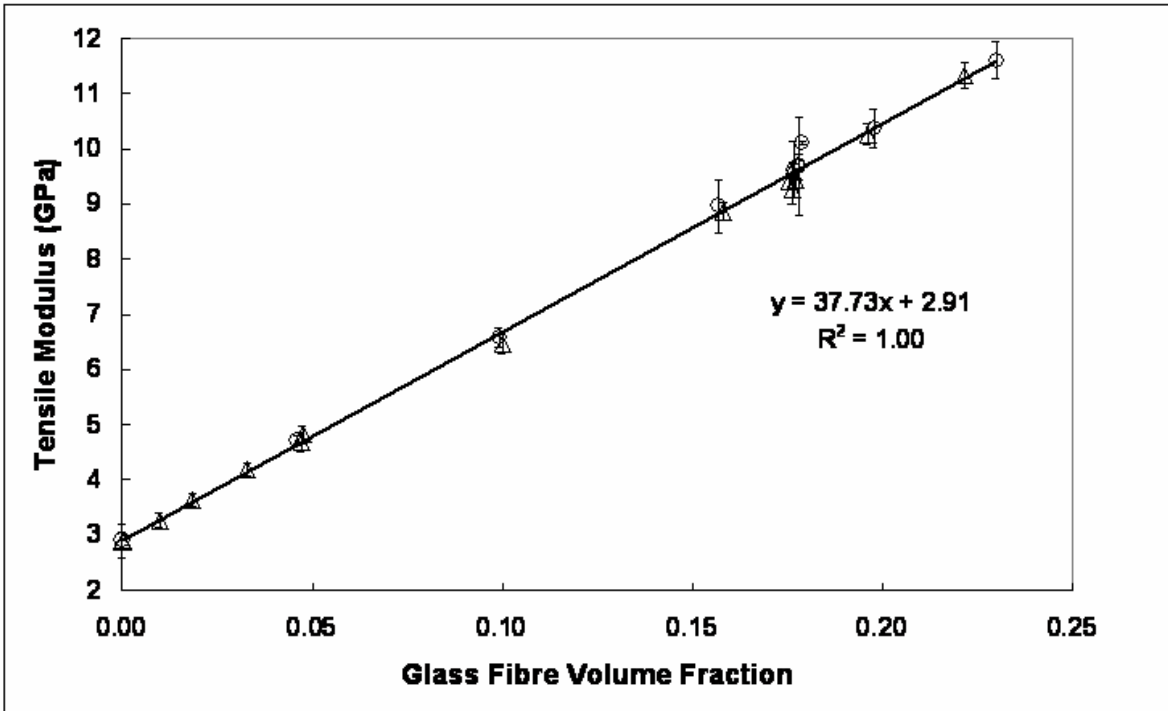
Figure 2 Tensile Modulus vs Fibre Volume Fraction (○ series A, △ series B)
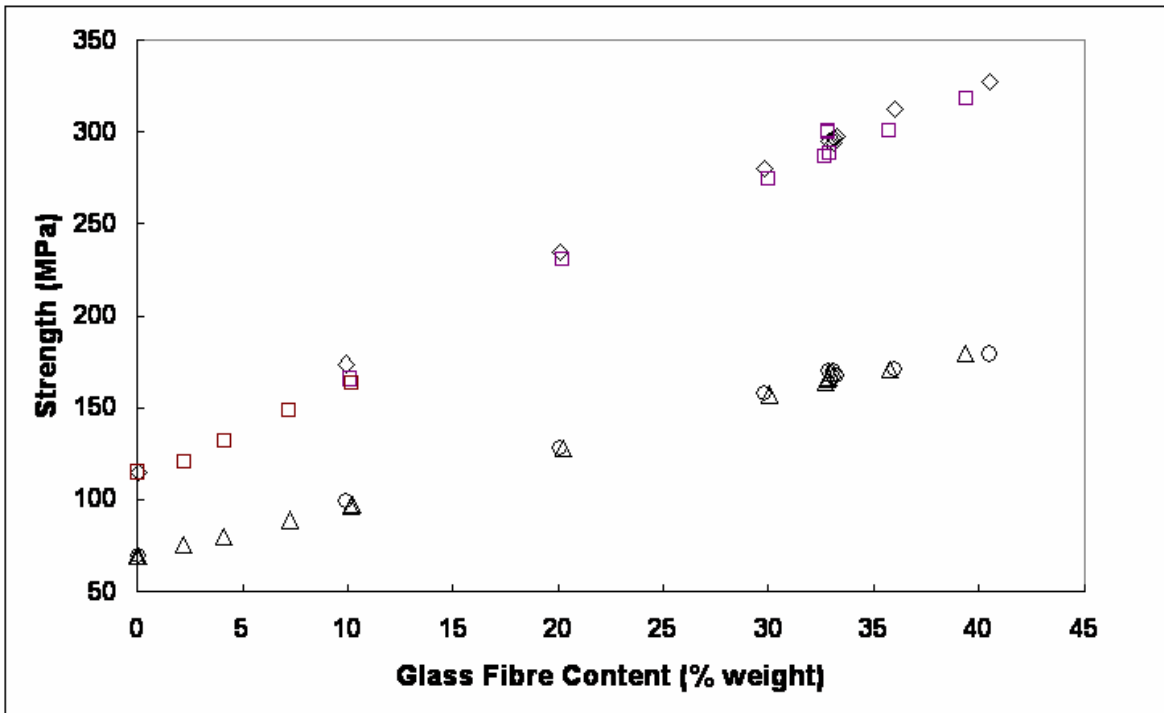
Figure 3 Composites Strengths vs Fibre Weight Content (◯ A tensile, △ B tensile, ◇ A flex, ☐ B flex)
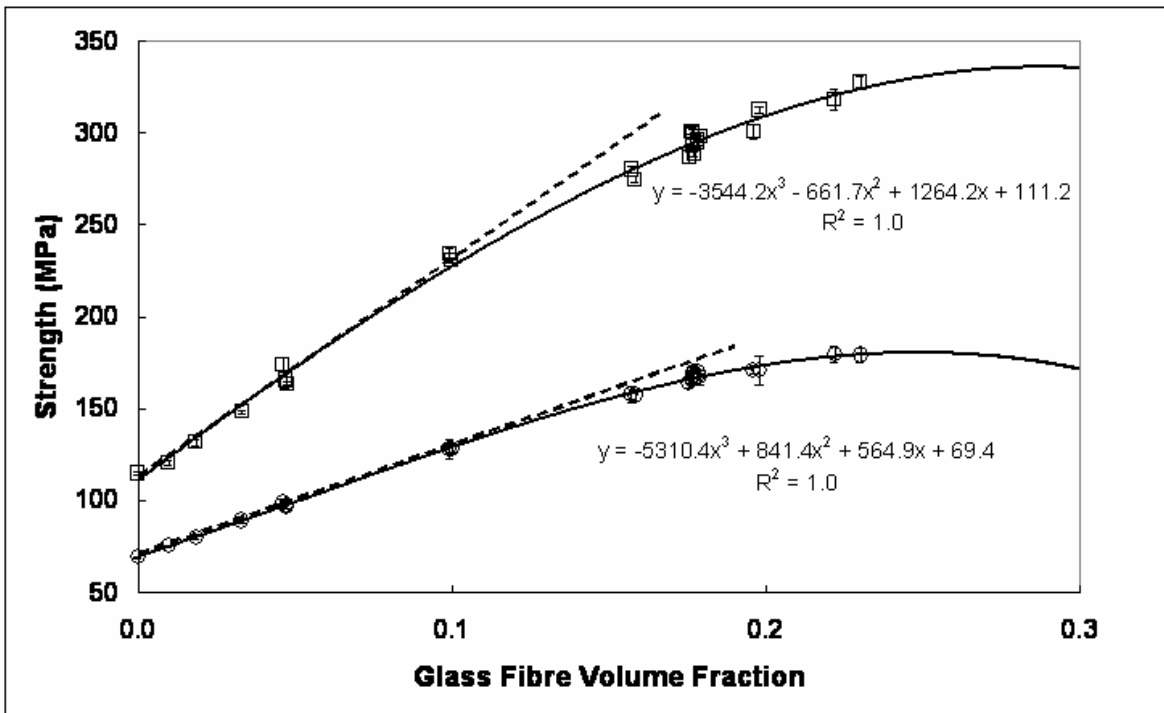
Figure 4 Composite Strengths vs Fibre Volume Fraction (◯ tensile, ☐ flex)

15
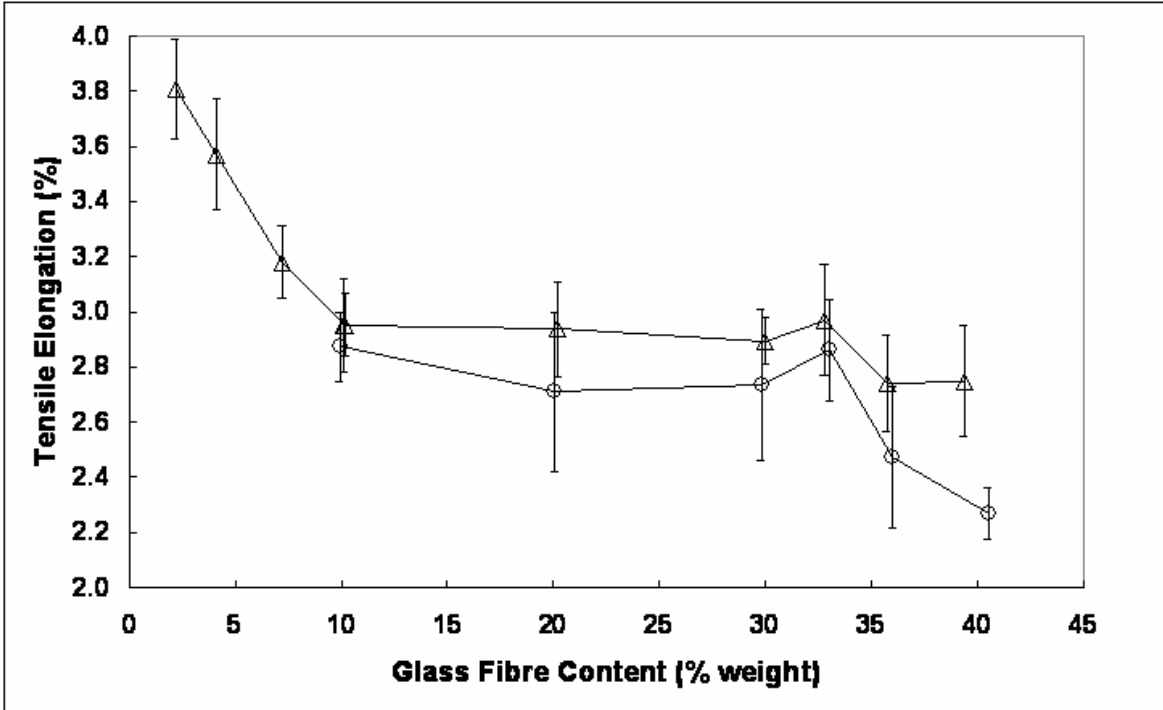
Figure 5 Tensile Elongation vs Fibre Weight Content (○ A, △ B)
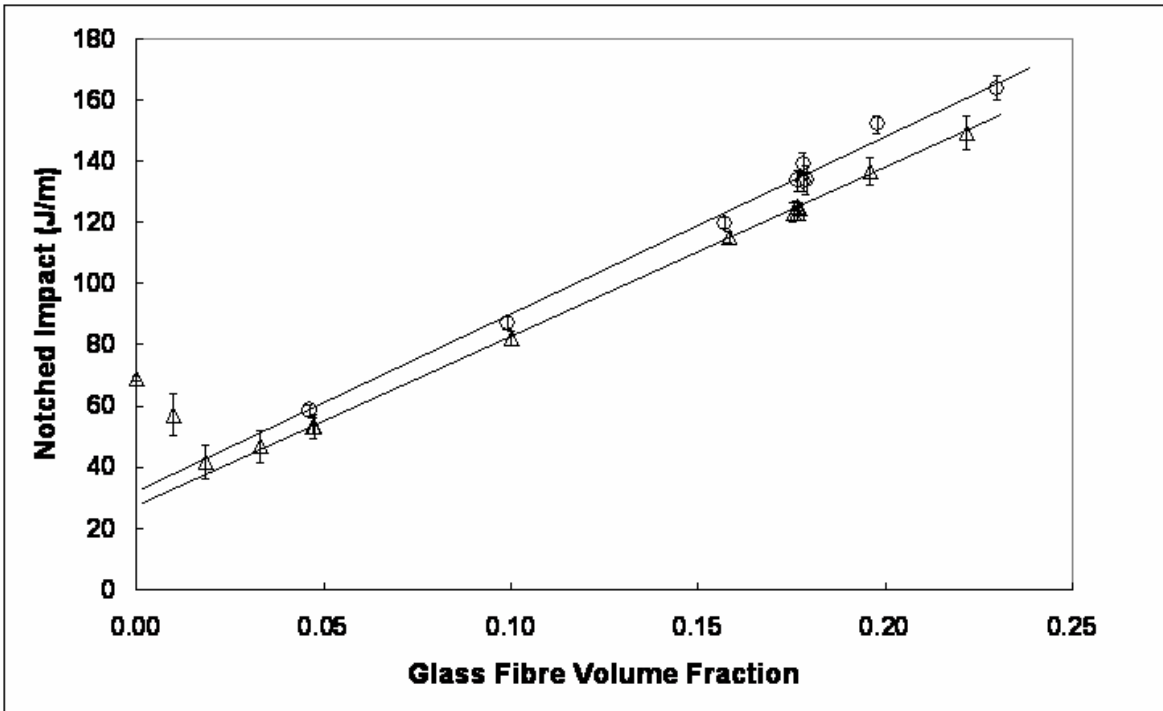
Figure 6 Notched Izod vs Fibre Volume Fraction (○ A, △ B)
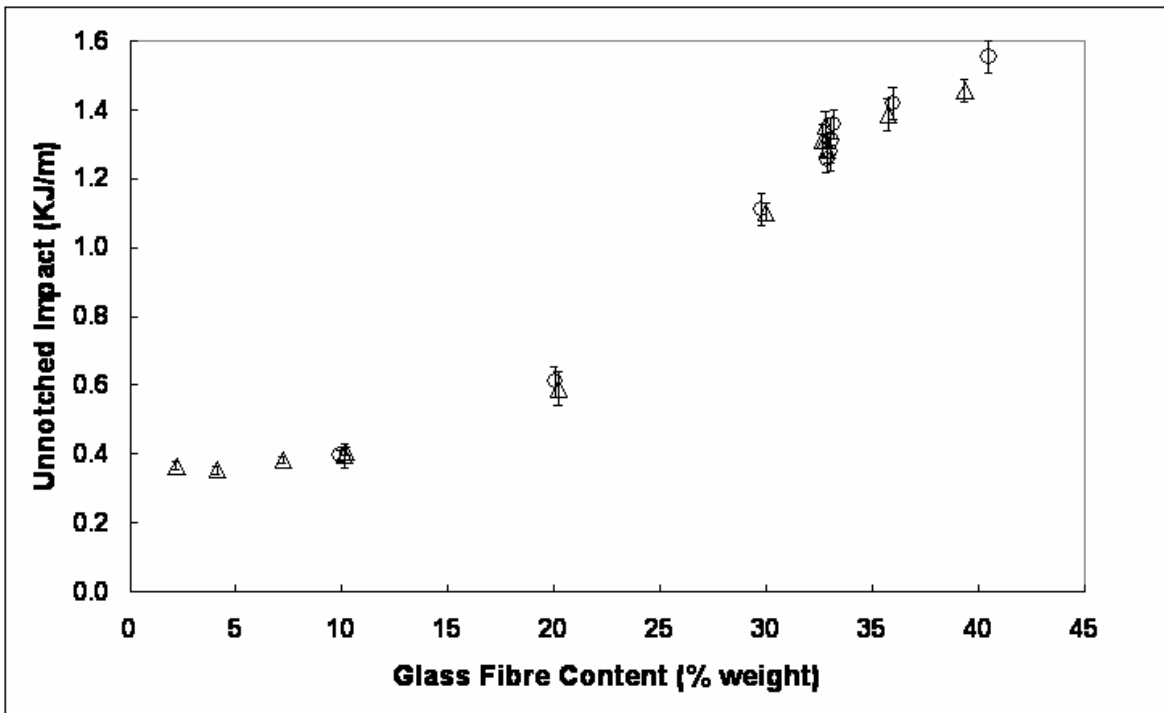
Figure 7 Unnotched Izod vs Fibre Weight Content (○ A, △ B)
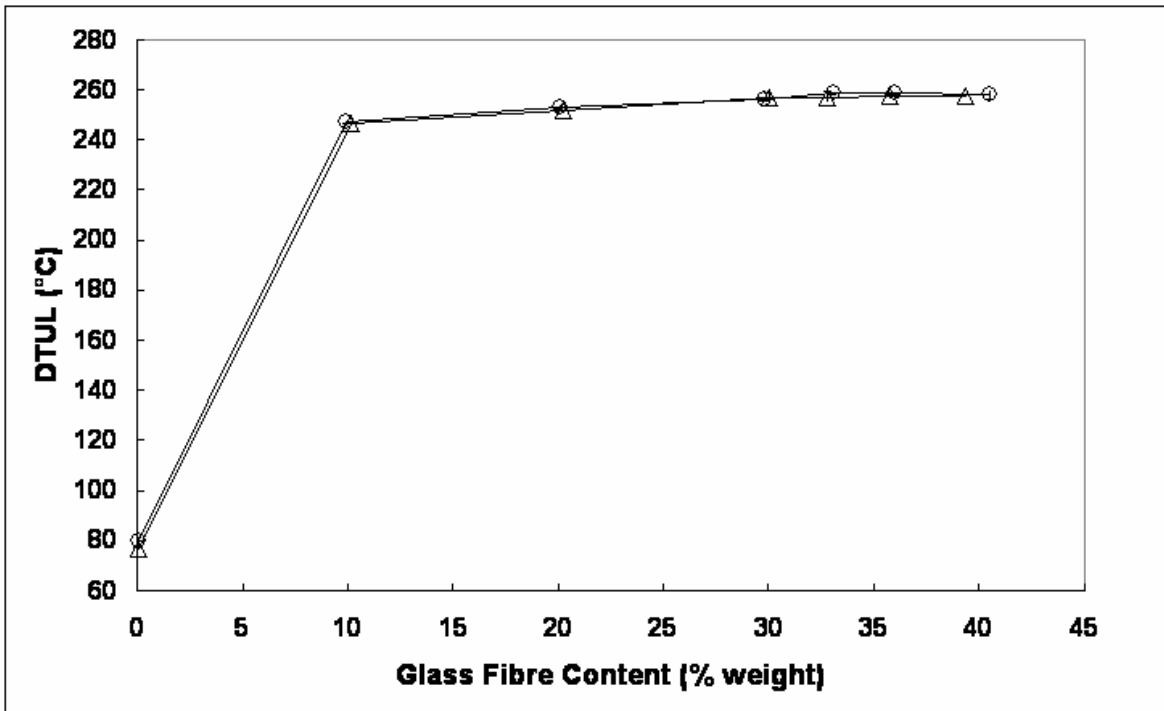
Figure 8 DTUL vs Fibre Weight Content (○ A, △ B)
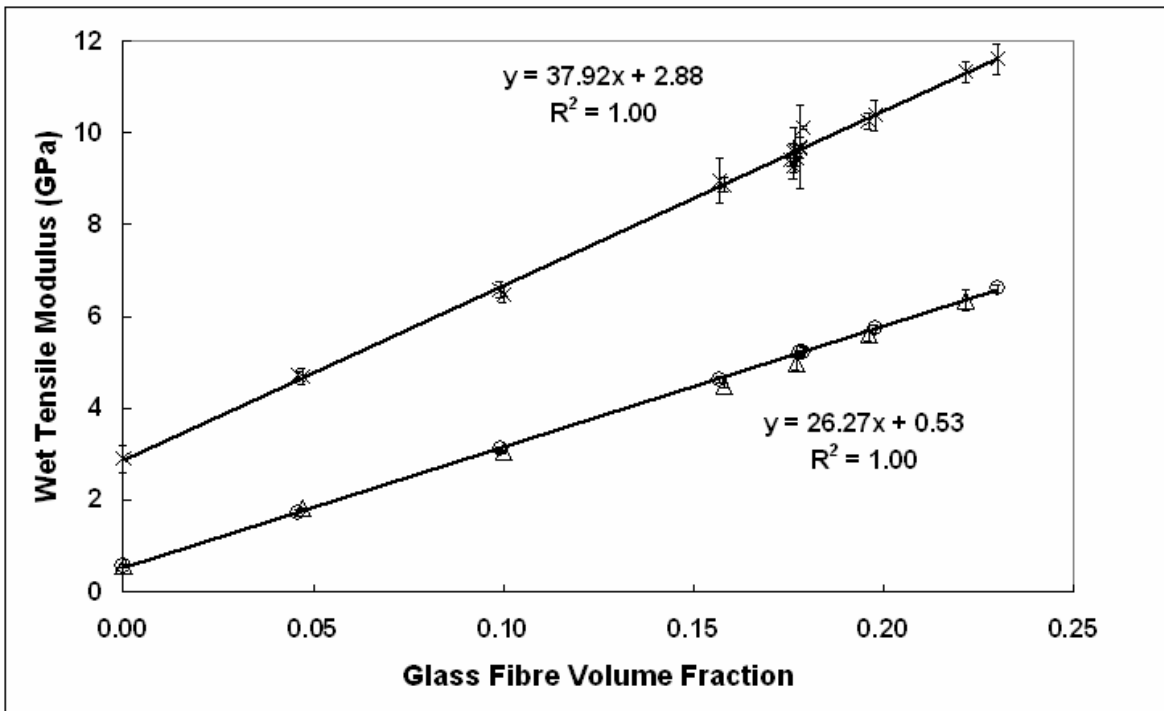
Figure 9 Wet Tensile Modulus vs Fibre Volume Fraction ($\times$ DaM, $\bigcirc$ A, $\triangle$ B)
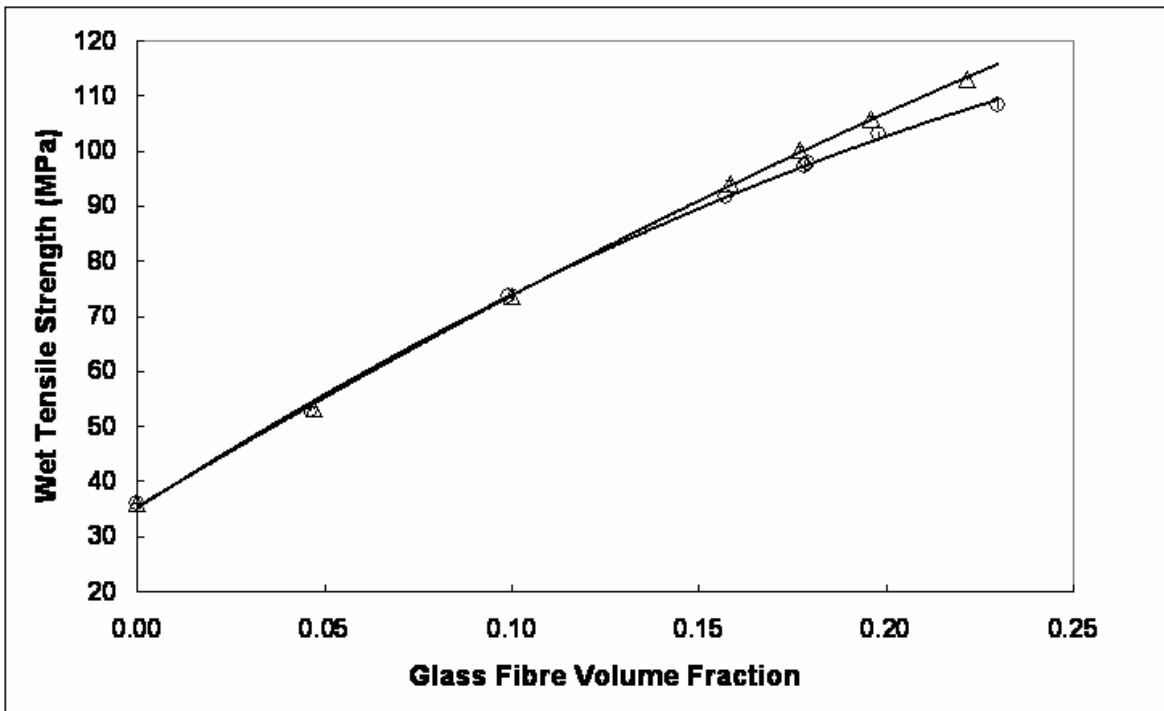
Figure 10 Wet Tensile Strength vs Fibre Volume Fraction ($\bigcirc$ A, $\triangle$ B)
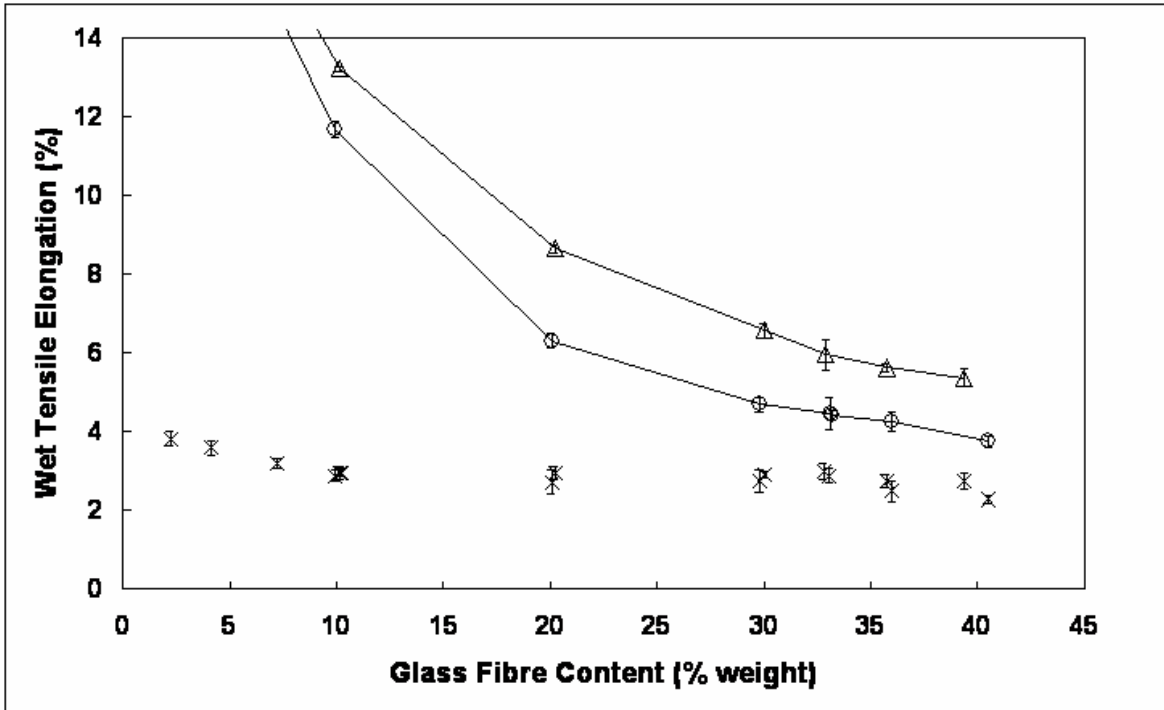
Figure 11 Wet Tensile Elongation vs Fibre Weight Content (× DaM, ○ A, △ B)
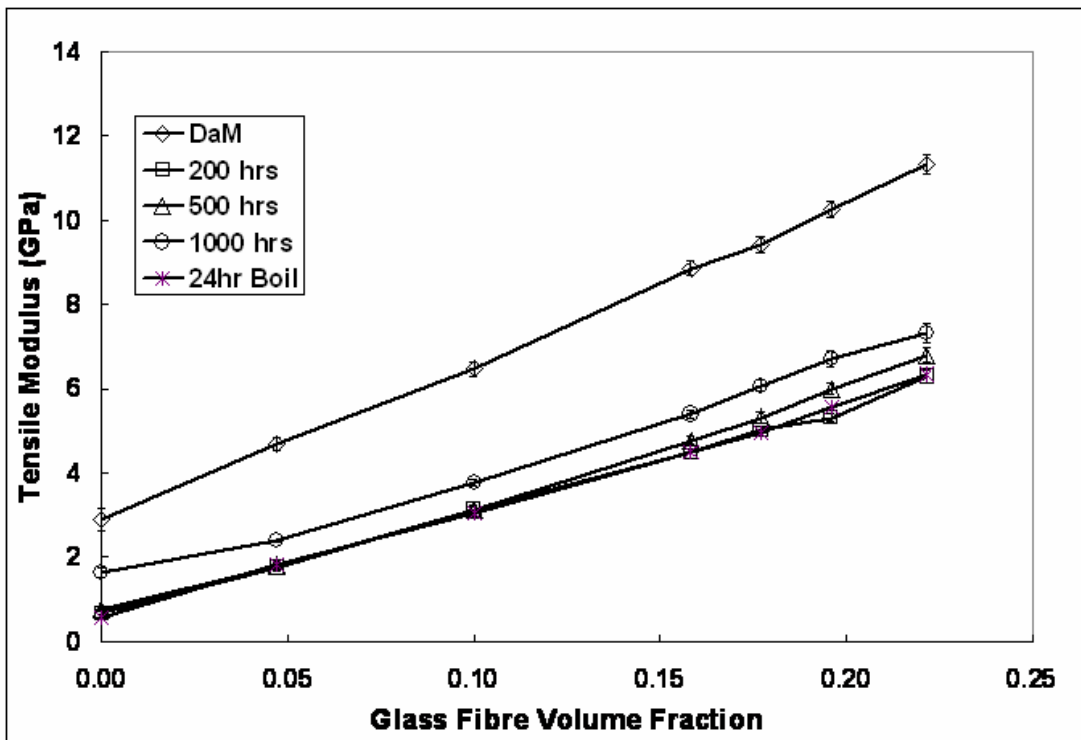
Figure 12 Hydrolysed Modulus vs Fibre Volume Fraction
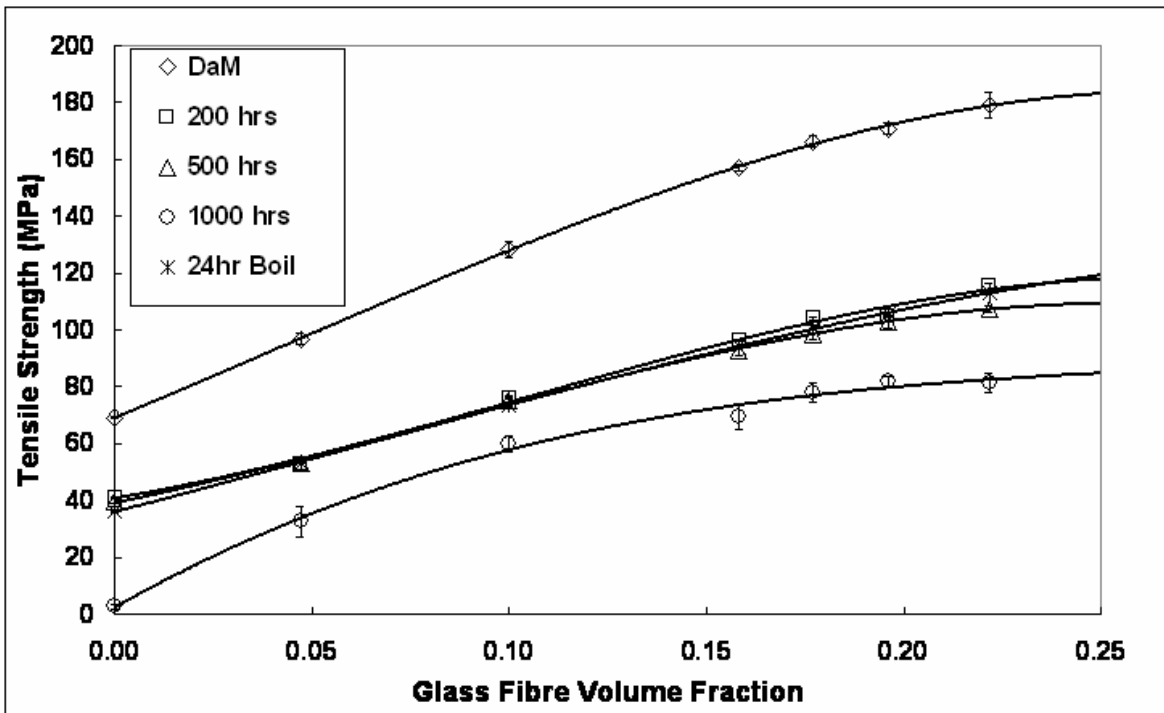
Figure 13 Tensile strength after hydroysis vs Fibre Volume Fraction
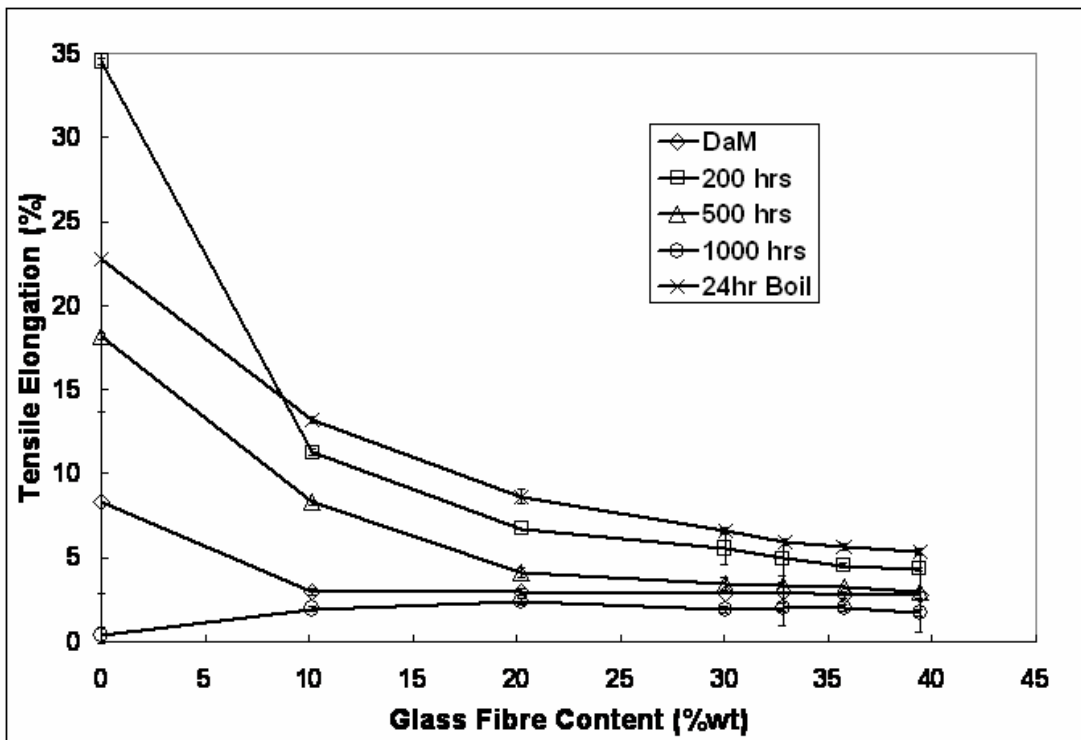
Figure 14 Elongation after hydrolysis vs Fibre Weight Content
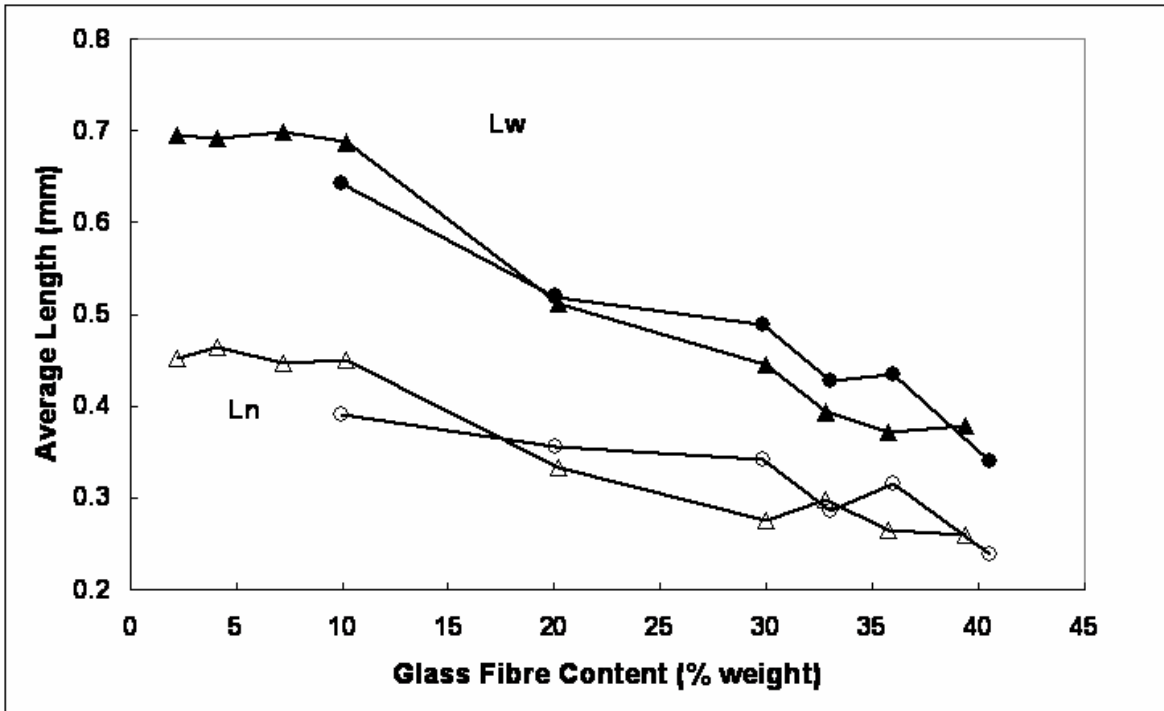
Figure15 Average Fibre Length vs Fibre Weight Content (○ A Ln, △ B Ln, (● A Lw, ▲ B Lw)
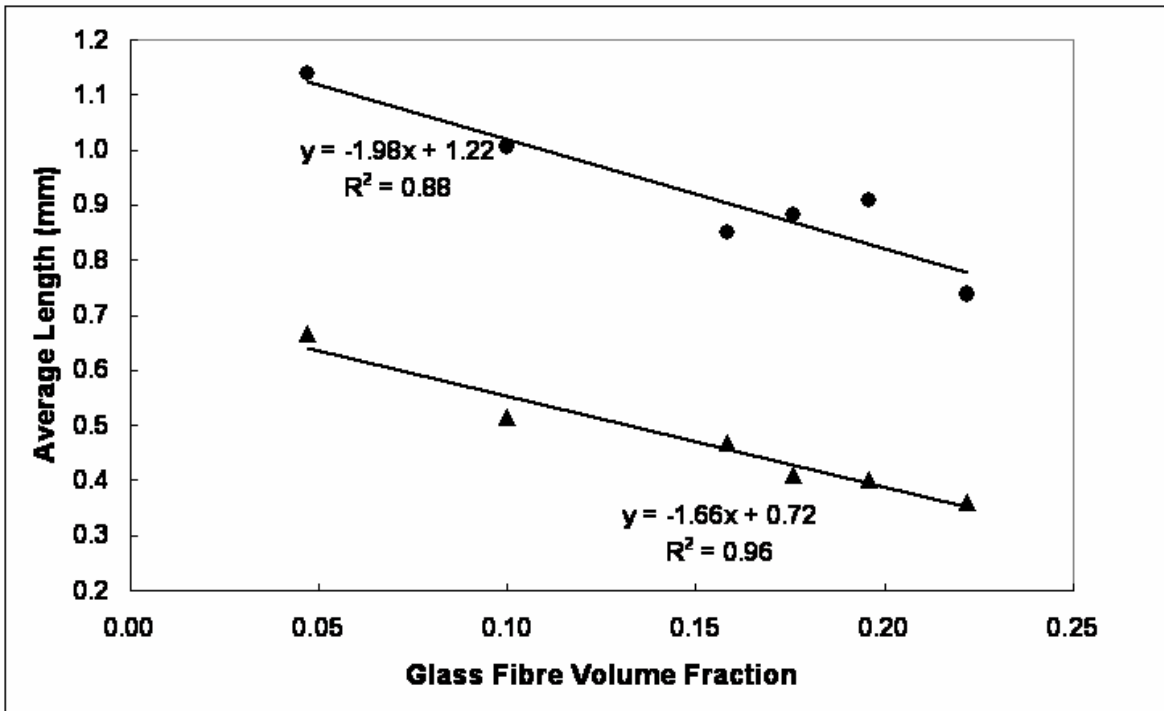
Figure 16 Fibre Length vs Fibre Volume Fraction (● extruded, ▲ moulded)
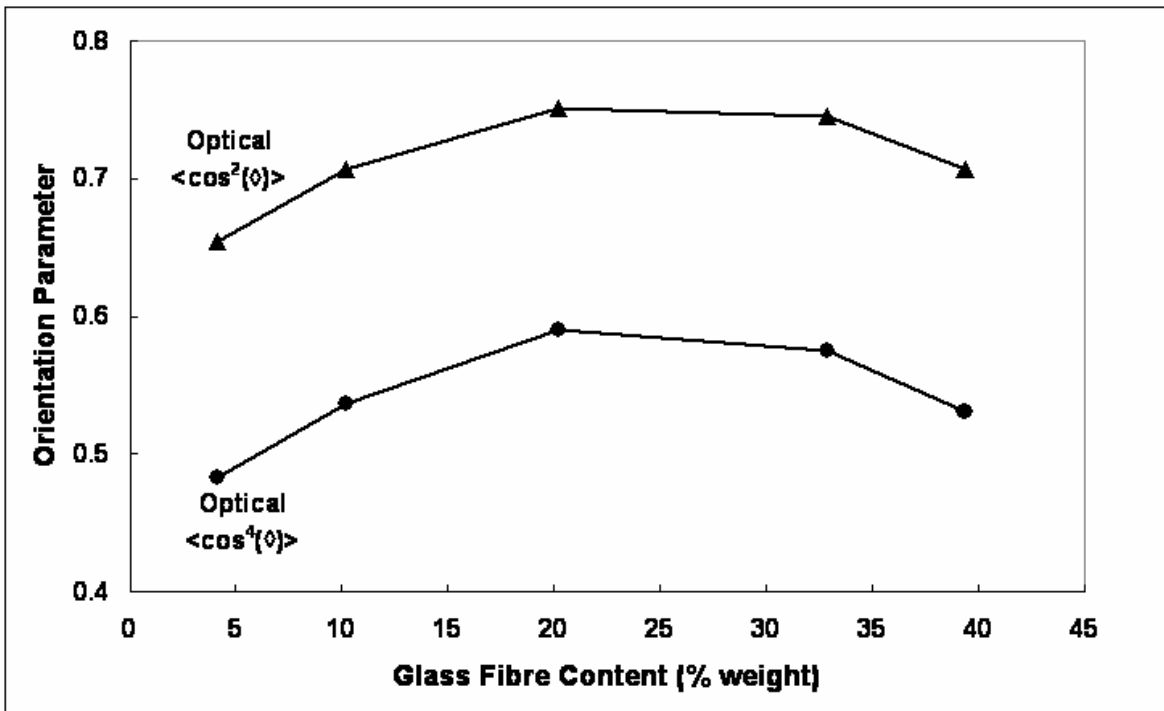
Figure 17 Fibre orientation vs Fibre Weight
Content
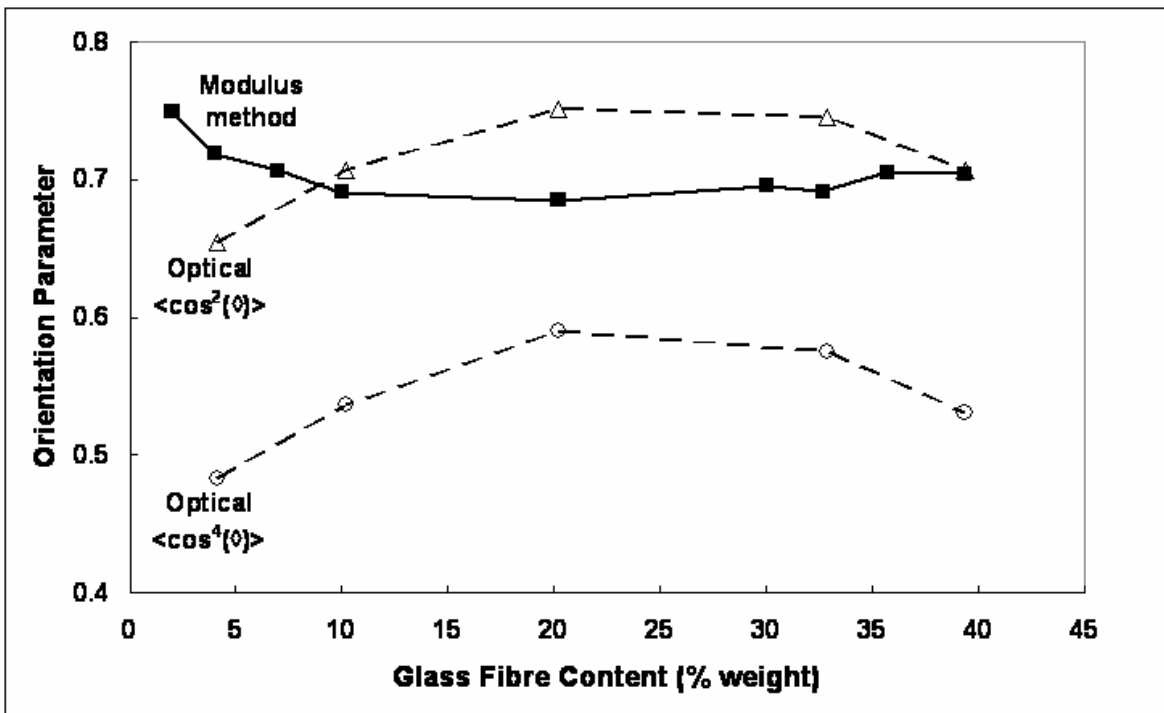
Figure 18 Orientation Factor vs Fibre Weight Content
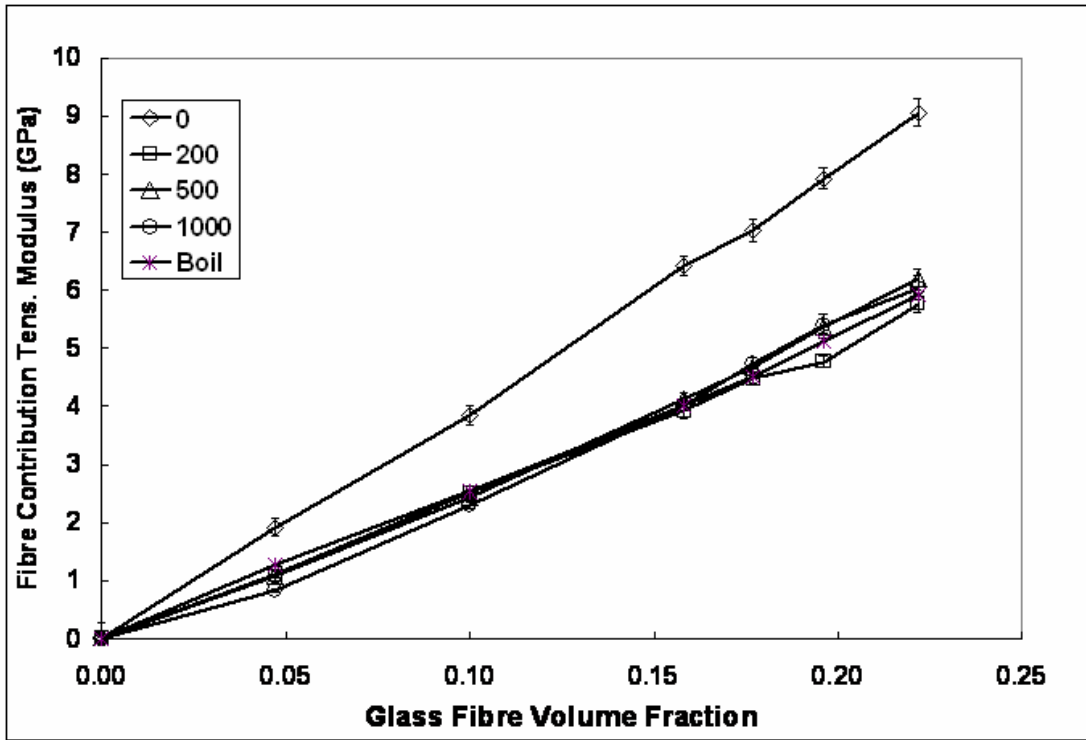
Figure 19 Fibre Contribution to Modulus vs Fibre Weight Content
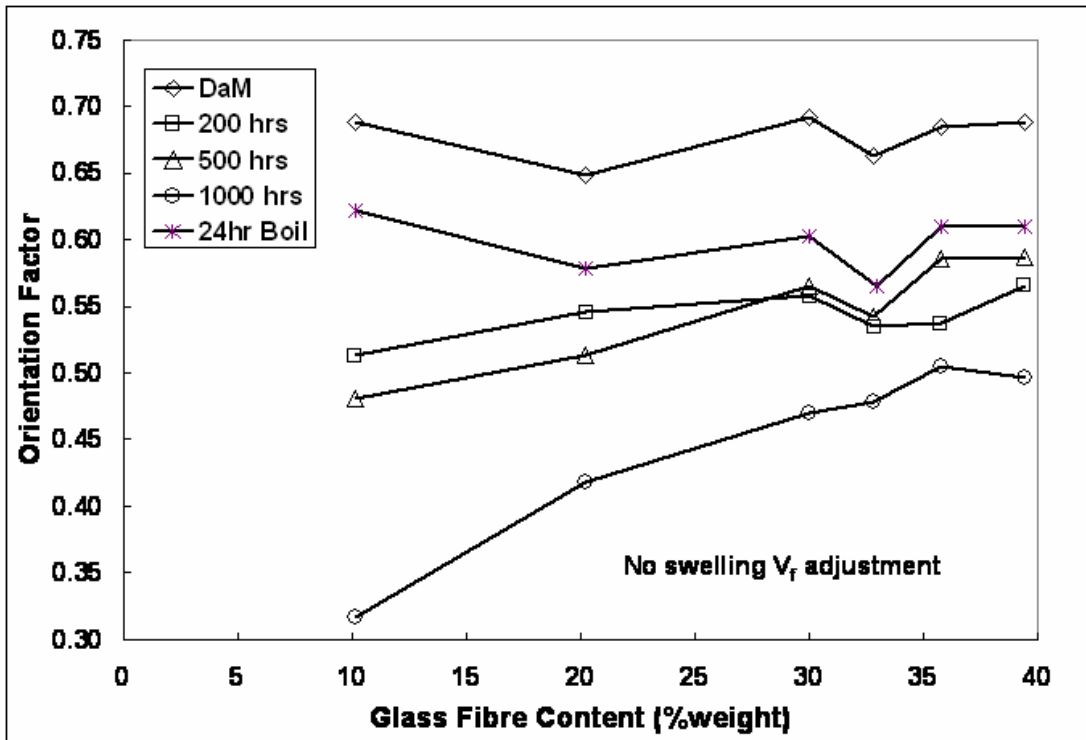
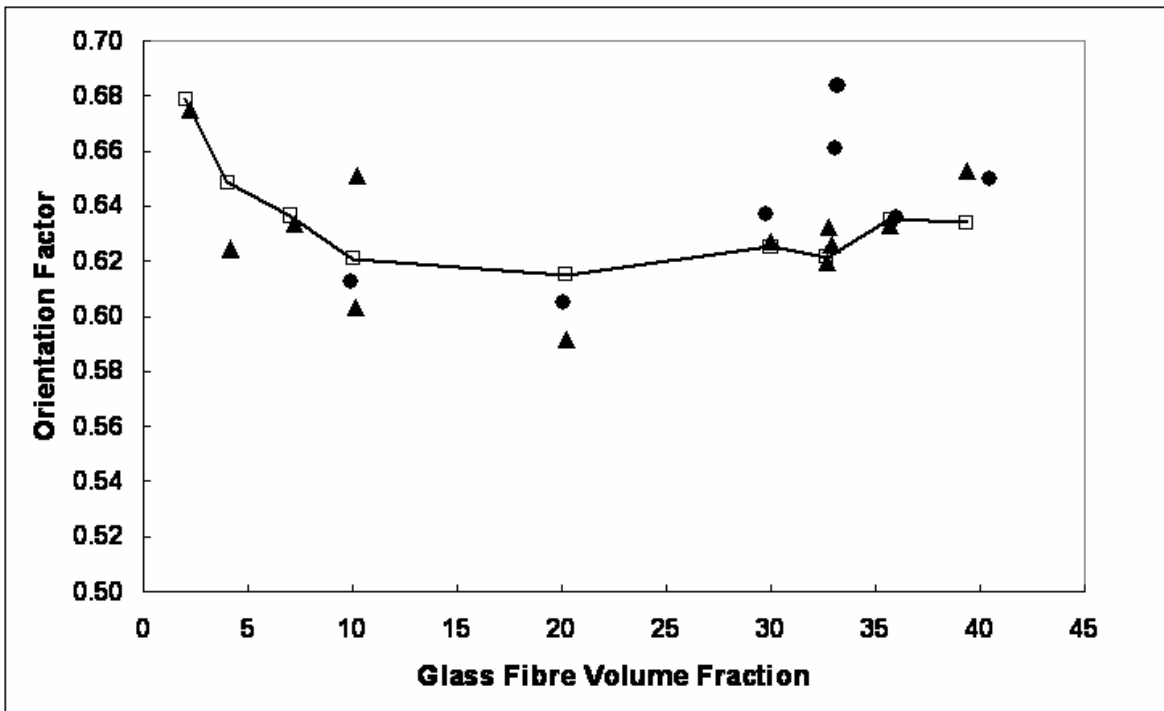Figure 20 Orientation Factor from Modulus vs Fibre Weight Content
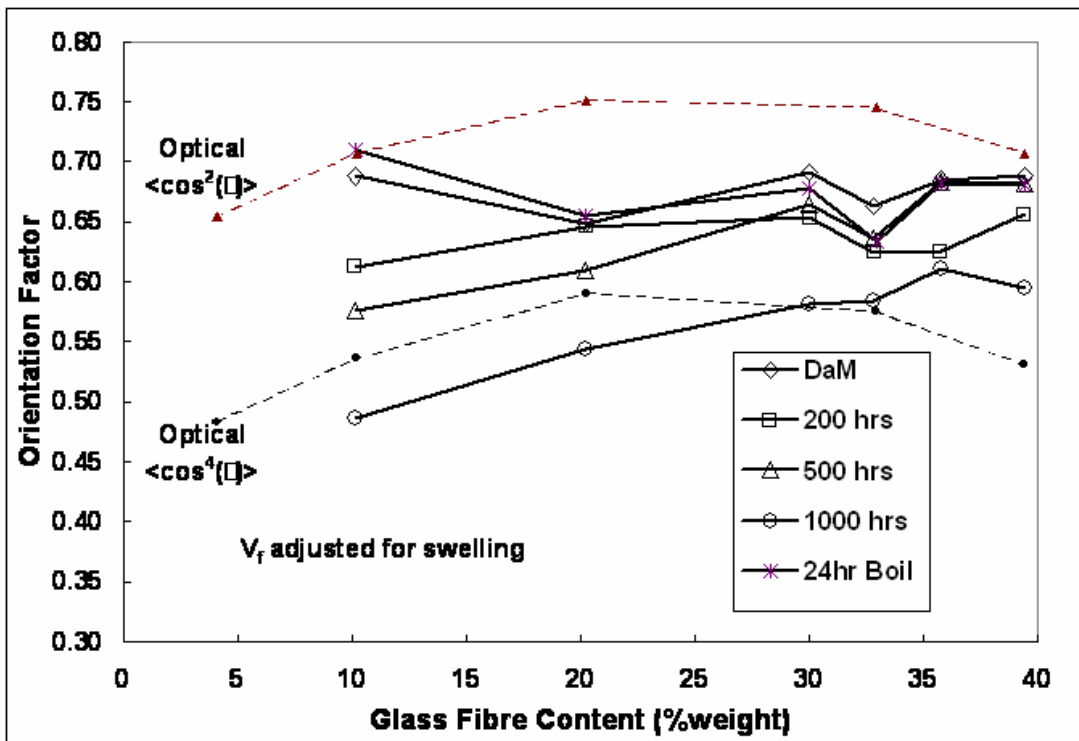
Figure 21 Orientation Factor from Modulus vs Fibre Weight Content
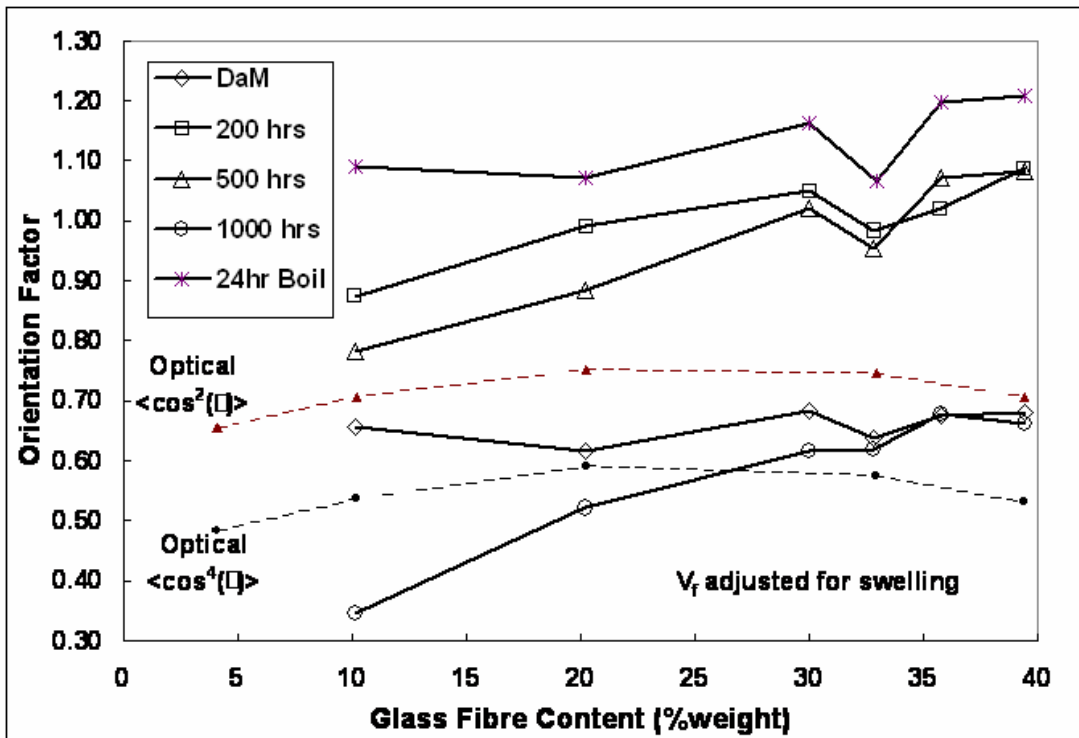
Figure 22 Orientation Factor from Modulus vs Fibre Weight Content

Figure 23 Orientation Factor from Macromodel vs Fibre Volume Fraction (● A, ▲ B, □ modulus)
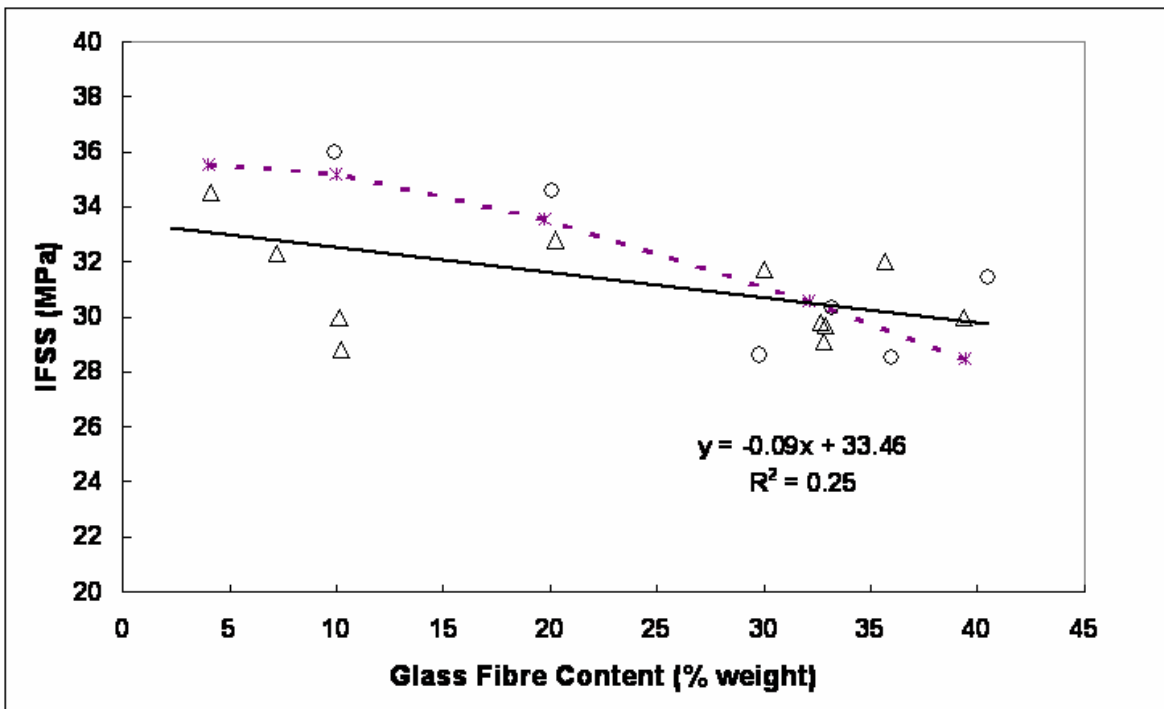

Figure 24 Interface strength vs Fibre Weight Content (○ A, △ B, ✳ theory)
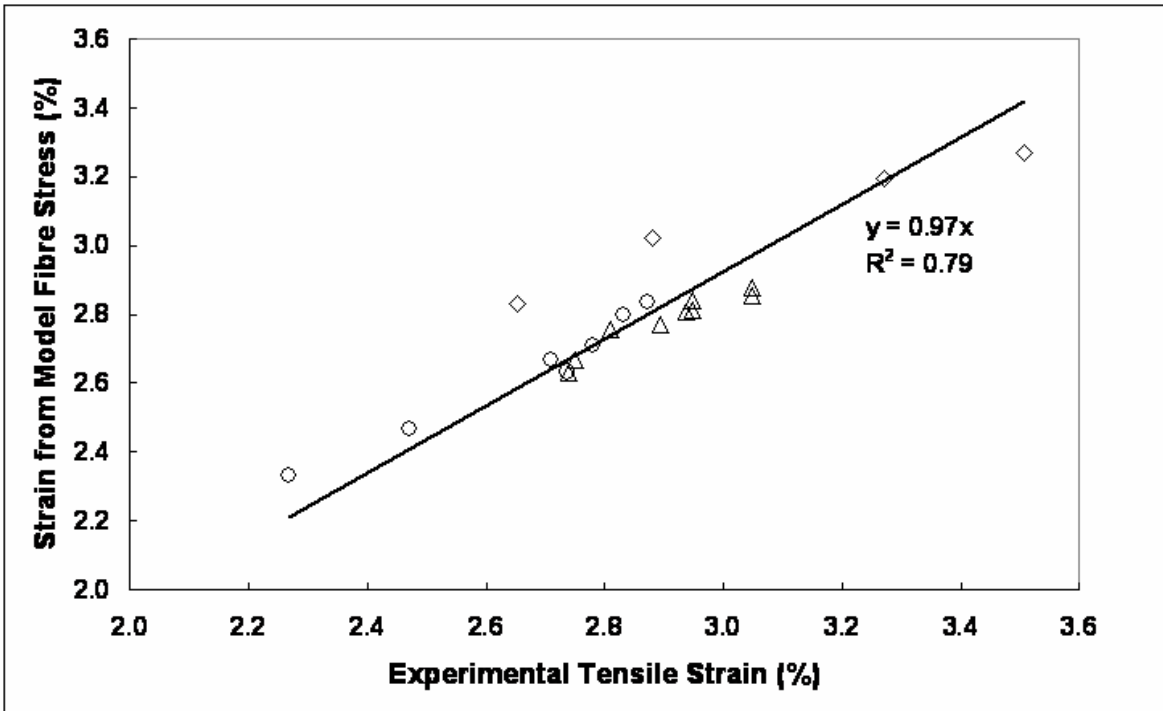
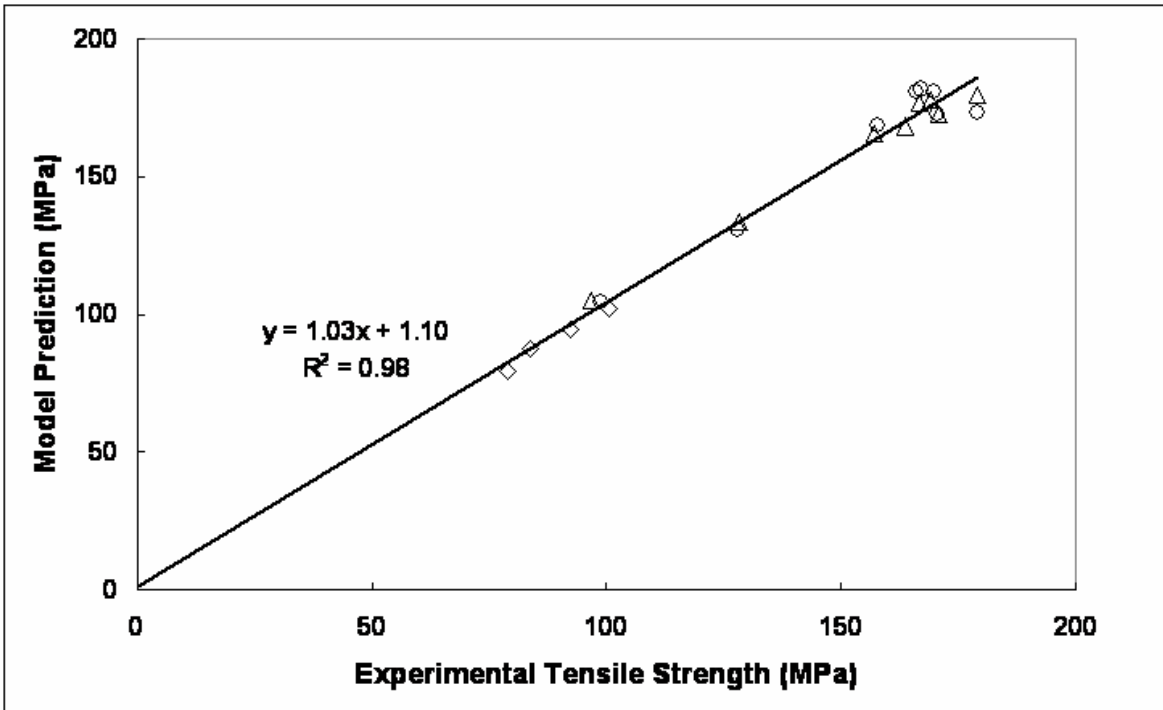Figure 25 Comparison Strain from Model vs Experiment (○ A , △ B1, ◇ B2)

Figure 26 Comparison Predicted Tensile Strength vs Experimental Value (○ A, △ B1, ◇ B2)